

# Self-Healing Hydrogel of Methotrexate-Loaded Nanoparticles Using *Artocarpus heterophyllus* Gum for Targeted Colon Cancer Therapy

Shruti Srivastav<sup>1</sup>, Abhilasha Singh<sup>1</sup>, Preeti Kush<sup>1\*</sup>, Manjul Pratap Singh<sup>2</sup>

<sup>1</sup>Adarsh Vijendra Institute of Pharmaceutical Sciences, Shobhit University, Gangoh, Saharanpur - 247 341, India.

<sup>2</sup>Vishveshwarya Group of Institutions, Abdul Kalam Technical University, Gautam Buddha Nagar - 201 314, India.

\*Corresponding author- Preeti Kush, e-mail: [preetikush85@gmail.com](mailto:preetikush85@gmail.com)

---

## Abstract

**Background:** Colon cancer remains a major cause of cancer-related morbidity and mortality worldwide, with conventional chemotherapy often hindered by poor specificity, systemic toxicity, and gastrointestinal degradation. Methotrexate (MTX), a widely used chemotherapeutic agent, suffers from limited oral bioavailability and non-targeted distribution. This study aimed to develop a pH-responsive, self-healing hydrogel system incorporating MTX-loaded PLGA nanoparticles using *Artocarpus heterophyllus* (jackfruit) seed gum for site-specific drug delivery to the colon.

**Methods:** MTX-loaded nanoparticles were formulated using the double emulsion solvent evaporation technique and characterized for particle size and polydispersity. A self-healing hydrogel was prepared via solution casting, combining jackfruit seed gum, chitosan, and polyvinyl alcohol, crosslinked with glutaraldehyde. MTX-loaded nanoparticles were embedded into the hydrogel matrix. The system was evaluated for swelling behavior, mechanical strength, self-healing efficiency, drug release, and structural properties using SEM, FTIR, and XRD techniques.

**Results:** The developed nanoparticles exhibited a mean size of  $85.6 \pm 4.5$  nm and a PDI of  $0.15 \pm 0.02$ . SEM revealed a porous hydrogel network with uniform nanoparticle distribution. FTIR confirmed successful chemical crosslinking and drug encapsulation, while XRD indicated drug amorphization within the matrix. The hydrogel demonstrated pH-sensitive swelling with a significantly higher swelling ratio at pH 7.4 ( $340\% \pm 10\%$ ) compared to pH 5.8 ( $200\% \pm 7\%$ ). Mechanical analysis showed a tensile strength of  $0.80 \pm 0.1$  MPa and  $90\% \pm 3\%$  self-healing efficiency. In vitro release studies confirmed colon-specific release, with 90% MTX released over 8 hours at pH 7.4, following non-Fickian kinetics. **Conclusion:** The jackfruit gum-based self-healing hydrogel system effectively encapsulates and delivers MTX in a controlled, colon-targeted manner while offering mechanical resilience and biocompatibility. This platform holds promise as a sustainable, site-specific oral chemotherapy strategy for improved colon cancer management.

**Keywords:** Colon cancer, methotrexate, nanoparticles, self-healing hydrogel, *Artocarpus heterophyllus*, PLGA, pH-responsive, controlled release.

---

## INTRODUCTION

Colon cancer stands as one of the most prevalent and life-threatening malignancies worldwide, posing a significant health burden despite notable advancements in screening and therapeutic interventions [1]. In its advanced stages, the prognosis remains grim, with low five-year survival rates [2]. Conventional chemotherapy, such as with methotrexate (MTX), targets rapidly dividing cells but lacks specificity, leading to severe side effects including nausea, immune suppression, and alopecia due to damage to healthy tissues like bone marrow and the gastrointestinal lining [3]. These drawbacks underscore the critical need for targeted, less toxic delivery strategies. The clinical efficacy of MTX is further undermined by its poor bioavailability, rapid systemic clearance, low solubility, and limited stability in the harsh gastrointestinal environment [4]. Oral delivery to the colon is particularly challenging due to degradation in the acidic stomach and enzymatic breakdown before reaching the intended site [5]. These limitations have sparked growing interest in novel delivery systems that can safeguard the drug, ensure site-specific release, and reduce collateral damage to non-cancerous tissues [6]. Hydrogels, especially self-healing types, have emerged as promising carriers due to their biocompatibility, stimulus-responsive release behavior, and tissue-like physical properties [7]. However, traditional hydrogels often lack mechanical resilience and

disintegrate under gut peristalsis [8]. Self-healing hydrogels, equipped with reversible bonds such as hydrogen or ionic interactions, overcome this limitation by restoring structural integrity post-disruption [9]. They provide sustained protection to encapsulated drugs throughout the digestive tract and are particularly well-suited for colon-targeted therapy [10]. The integration of nanoparticles (NPs) within hydrogels further elevates their potential. NPs offer controlled, pH-sensitive drug release, extended circulation times, and tumor-specific targeting via surface modifications, taking advantage of the enhanced permeability and retention (EPR) effect in tumor tissues [11]. Within a hydrogel matrix, NPs act as precision tools, reaching and penetrating cancerous tissues while minimizing systemic toxicity [12]. A noteworthy innovation lies in utilizing *Artocarpus heterophyllus* (jackfruit) gum—a natural, polysaccharide-rich, biodegradable, and biocompatible material—as the hydrogel base [13]. This plant-derived polymer brings additional advantages such as sustainability, cost-effectiveness, and mucoadhesive or gel-forming capabilities, aligning with green pharmaceutical practices [14]. The formulation of a self-healing hydrogel embedded with MTX-loaded NPs using jackfruit gum thus emerges from a well-defined clinical and scientific rationale. It addresses current therapeutic limitations by ensuring MTX is shielded through the stomach and small intestine, releasing only at the colon's higher pH environment, enhancing therapeutic precision while minimizing side effects [10]. The hydrogel's self-healing nature ensures it survives mechanical and chemical challenges within the gut, providing sustained and localized drug release [9]. Functionalized nanoparticles further optimize this system by enabling smart, pH-responsive drug liberation and targeted uptake by colon cancer cells, reducing off-target effects [12]. The incorporation of jackfruit gum not only enhances the safety profile but also supports affordability and ecological responsibility in pharmaceutical development [13]. This multifaceted approach builds upon existing studies on natural polymers and self-healing materials, integrating disciplines like materials science, oncology, and pharmacology to advance colon cancer therapy [14]. Nonetheless, several challenges must be addressed, including ensuring hydrogel stability in the upper GI tract, refining NP targeting specificity, and scaling up production in a cost-effective and regulatory-compliant manner [6]. Despite these potential obstacles, the promise of improved therapeutic outcomes, reduced adverse effects, and sustainable innovation makes this system a compelling frontier in colon cancer drug delivery [1, 14].

## MATERIALS AND METHODS

### Materials

#### Chemicals and Reagents:

Methotrexate (MTX) was obtained from Sigma-Aldrich (St. Louis, MO, USA). Poly(D,L-lactide-co-glycolide) (PLGA; 50:50, MW 30,000–60,000), polyvinyl alcohol (PVA, MW 89,000–98,000), and glutaraldehyde (25% aqueous solution) were also procured from Sigma-Aldrich. Chitosan (CS, medium molecular weight, degree of deacetylation ~85%) and dichloromethane (analytical grade) were purchased from HiMedia Laboratories Pvt. Ltd. (Mumbai, India). Phosphate-buffered saline (PBS, pH 7.4) and acetic acid (glacial, AR grade) were obtained from Merck (India). All other chemicals and reagents used were of analytical grade and used without further purification.

#### Plant Material:

Fresh seeds of *Artocarpus heterophyllus* (jackfruit) were collected from a local fruit market in Ghaziabad, Uttar Pradesh, India, during the peak ripening season (June–July). The seeds were washed thoroughly with distilled water to remove any adhering pulp or debris and air-dried at room temperature ( $25 \pm 2^\circ\text{C}$ ) for 7 days. The dried seeds were then pulverized using a mechanical grinder (REMI, India) and sieved to obtain fine seed flour. The flour was stored in a desiccator until further use [15].

#### Extraction of Gum from *Artocarpus heterophyllus* Seeds:

The extraction of gum was performed using a previously reported protocol with slight modifications. Briefly, 100 g of jackfruit seed flour was subjected to maceration in 500 mL of 95% ethanol for defatting over 24 hours. The residue was air-dried and extracted using distilled water (1:10 w/v) under continuous magnetic stirring at  $70^\circ\text{C}$  for 4 hours. The hot extract was filtered through muslin cloth and centrifuged at 6000 rpm for 15 minutes. The supernatant was precipitated using three volumes of chilled acetone. The precipitated gum was collected, dried at  $40^\circ\text{C}$  in a hot air oven, powdered, and stored in airtight containers for further formulation work [16].

## Nanoparticle Synthesis

### Preparation of MTX-Loaded PLGA Nanoparticles:

Methotrexate (MTX)-loaded nanoparticles were synthesized using a double emulsion (water-in-oil-in-water, W/O/W) solvent evaporation method, widely used for encapsulating hydrophilic drugs into polymeric matrices such as PLGA. Briefly, 10 mg of MTX was dissolved in 1 mL of phosphate-buffered saline (PBS, pH 7.4) to form the inner aqueous phase ( $W_1$ ). This solution was then emulsified into 5 mL of dichloromethane containing 100 mg of PLGA (50:50, MW  $\sim$  40,000), serving as the organic phase (O). The primary emulsion ( $W_1/O$ ) was generated by probe sonication (VCX 750, Sonics & Materials Inc., USA) at 40% amplitude for 60 seconds in an ice bath. This primary emulsion was then added dropwise into 20 mL of 2% (w/v) aqueous PVA solution (external aqueous phase,  $W_2$ ) under high-speed homogenization (Ultra-Turrax T25, IKA, Germany) at 10,000 rpm for 5 minutes, followed by sonication at 40% amplitude for 1 minute to form a stable W/O/W emulsion. The resulting emulsion was stirred at room temperature under reduced pressure (using a rotary evaporator) to allow solvent evaporation and nanoparticle solidification. The formed nanoparticles were recovered by centrifugation at 15,000 rpm for 20 minutes at 4°C (REMI C-24BL, India), washed three times with distilled water to remove residual PVA and unencapsulated drug, and finally lyophilized (Labconco FreeZone) with 5% trehalose as cryoprotectant. The dried nanoparticles were stored in airtight vials at 4°C for further incorporation into the hydrogel matrix [17].

### Hydrogel Preparation

#### Formulation of MTX-Nanoparticle Loaded Self-Healing Hydrogel:

The hydrogel matrix was prepared using a solution casting technique, employing *Artocarpus heterophyllus* seed gum as the primary polymer, blended with chitosan (CS) and polyvinyl alcohol (PVA) to enhance mechanical strength and mucoadhesiveness. Initially, 1% w/v jackfruit seed gum was dispersed in distilled water and heated at 60°C for 1 hour with continuous magnetic stirring to ensure complete hydration and swelling. In parallel, 1% w/v chitosan was dissolved in 1% v/v glacial acetic acid under mild heating (50°C) and stirred until a clear solution was obtained. Separately, 5% w/v PVA was dissolved in hot distilled water at 90°C, followed by cooling to room temperature. These three polymer solutions were mixed in a 1:1:1 ratio under continuous stirring at 37°C for 2 hours to form a homogenous polymer blend. To this blend, 0.1% v/v glutaraldehyde (25% aqueous solution) was added slowly as a covalent crosslinker under gentle stirring, and the pH was maintained at 4.5 using 0.1N HCl or NaOH, promoting efficient crosslinking between hydroxyl and amino groups of the polymers. Subsequently, 10 mg/mL of lyophilized MTX-loaded PLGA nanoparticles were dispersed uniformly into the hydrogel base using a vortex mixer followed by mild ultrasonication (15 sec) to avoid agglomeration. The final hydrogel mixture was then poured into Teflon-coated molds and allowed to air dry at 40°C for 24 hours to form thin hydrogel films. The dried hydrogels were peeled off and stored under vacuum in a desiccator at room temperature until further use. The hydrogel matrix was designed to possess self-healing characteristics through reversible hydrogen bonding and ionic interactions, facilitating its structural recovery upon mechanical damage, and enabling colon-specific drug release [17].

## CHARACTERIZATION

### 1. Morphological Analysis (SEM)

The surface morphology and internal structure of the MTX-loaded hydrogel films were examined using Scanning Electron Microscopy (SEM) (JEOL JSM-7610F, Japan). Hydrogel samples were cut into small pieces, mounted on aluminum stubs using carbon tape, and sputter-coated with gold under vacuum using a sputter coater (Quorum Q150R). Images were captured at different magnifications (500 $\times$ –5000 $\times$ ) under an accelerating voltage of 15 kV to observe porosity, pore distribution, and nanoparticle embedding [18].

### 2. Fourier Transform Infrared Spectroscopy (FTIR)

FTIR spectra were recorded to identify characteristic functional groups and confirm crosslinking interactions between polymers and drug molecules. Dried samples of pure MTX, PLGA, jackfruit gum, blank hydrogel, and drug-loaded hydrogel were scanned using an FTIR spectrophotometer (PerkinElmer

Spectrum Two) in the range of 4000–400  $\text{cm}^{-1}$  using the KBr pellet method. Key peaks were analyzed to detect hydrogen bonding, ester, amine, and aldehyde group interactions [19].

### 3. X-ray Diffraction (XRD)

XRD analysis was carried out to assess the crystalline or amorphous nature of MTX in the hydrogel matrix using an X-ray diffractometer (Bruker D8 Advance) with Cu-K $\alpha$  radiation ( $\lambda = 1.5406 \text{ \AA}$ ). The diffractograms were recorded in the  $2\theta$  range of  $5^\circ$  to  $50^\circ$  at a scanning rate of  $2^\circ/\text{min}$ . The disappearance or broadening of MTX peaks was interpreted as evidence of molecular dispersion and amorphization [20].

### 4. Swelling Behavior

Swelling studies were performed to evaluate the pH and temperature responsiveness of the hydrogels. Pre-weighed dry hydrogel discs ( $W_0$ ) were immersed in phosphate-buffered saline (PBS) at pH 5.8 and pH 7.4, and temperatures of  $37^\circ\text{C}$  and  $43^\circ\text{C}$ . After 24 hours, the swollen hydrogels were removed, surface blotted, and weighed ( $W_t$ ). The swelling ratio (%) was calculated using the formula:

$$\text{Swelling ratio (\%)} = ((W_t - W_0) / W_0) \times 100$$

Each experiment was performed in triplicate ( $n = 3$ ), and mean  $\pm$  SD values were reported.

### 5. Mechanical Properties and Self-Healing Efficiency

Mechanical strength and flexibility of the hydrogels were evaluated using a texture analyzer (TA.XT Plus, Stable Micro Systems, UK). The tensile strength and percentage elongation at break were measured using rectangular strips ( $2 \text{ cm} \times 1 \text{ cm}$ ) at a crosshead speed of  $5 \text{ mm}/\text{min}$ . For self-healing studies, hydrogel samples were cut in half and gently pressed together under mild moisture conditions [20]. After 30 minutes, the healed hydrogel was again subjected to tensile testing. Self-healing efficiency (%) was calculated as:

$$\text{Efficiency (\%)} = (\text{Tensile strength of healed sample} / \text{Original tensile strength}) \times 100$$

### 6. Contact Angle Measurement

The hydrophilicity and mucoadhesive potential of the hydrogel surface were assessed by static water contact angle measurements using a contact angle goniometer (KRÜSS DSA25). A  $5 \mu\text{L}$  drop of distilled water was placed on the surface of the dried hydrogel film, and the contact angle was recorded within 10 seconds. A contact angle below  $40^\circ$  was considered indicative of strong hydrophilicity and potential for mucosal adhesion.

### 7. In Vitro Drug Release Studies

The release profile of MTX from the hydrogel was studied using USP Type II dissolution apparatus (paddle method). Hydrogel discs (equivalent to 1 mg MTX) were placed in 50 mL PBS at pH 5.8 and pH 7.4 at  $37 \pm 0.5^\circ\text{C}$ , stirred at 50 rpm. At predefined time intervals (0–12 h), 2 mL of sample was withdrawn and replaced with fresh medium. The samples were filtered and analyzed using a UV-Vis spectrophotometer (Shimadzu UV-1800) at  $\lambda = 303 \text{ nm}$ . Drug release kinetics were evaluated by fitting the data into zero-order, first-order, Higuchi, and Korsmeyer–Peppas models, and the release exponent ( $n$ ) was used to determine the mechanism [21].

## RESULTS AND DISCUSSION

### Physicochemical Properties of the MTX-Loaded Hydrogel System

The physicochemical characterization data presented in Table 1 highlight the robustness and colon-targeting suitability of the developed MTX-loaded hydrogel. The average nanoparticle size of  $85.6 \pm 4.5 \text{ nm}$ , with a low polydispersity index (PDI) of  $0.15 \pm 0.02$ , indicates a monodisperse system ideal for passive tumor targeting via the enhanced permeability and retention (EPR) effect. Nanoparticles of this size range are also favorable for efficient cellular uptake and prolonged circulation time in systemic drug delivery. The hydrogel exhibited distinct pH-responsive swelling behavior, with significantly higher swelling ratios at pH 7.4 ( $340\% \pm 10\%$ ) compared to pH 5.8 ( $200\% \pm 7\%$ ). This behavior is crucial for colon-specific delivery, as the higher pH environment of the colon activates the hydrogel matrix to swell and release its drug payload. The temperature responsiveness, reflected by an approximate 10% increase in swelling at  $43^\circ\text{C}$ , further supports the thermosensitive nature of the formulation, which may be beneficial in hyperthermic tumor microenvironments. The hydrogel demonstrated excellent mechanical strength and flexibility, with a tensile strength of  $0.80 \pm 0.1 \text{ MPa}$  and an elongation at break of  $140\% \pm 9\%$ . These values suggest adequate durability to withstand physiological peristalsis and mechanical stress in the

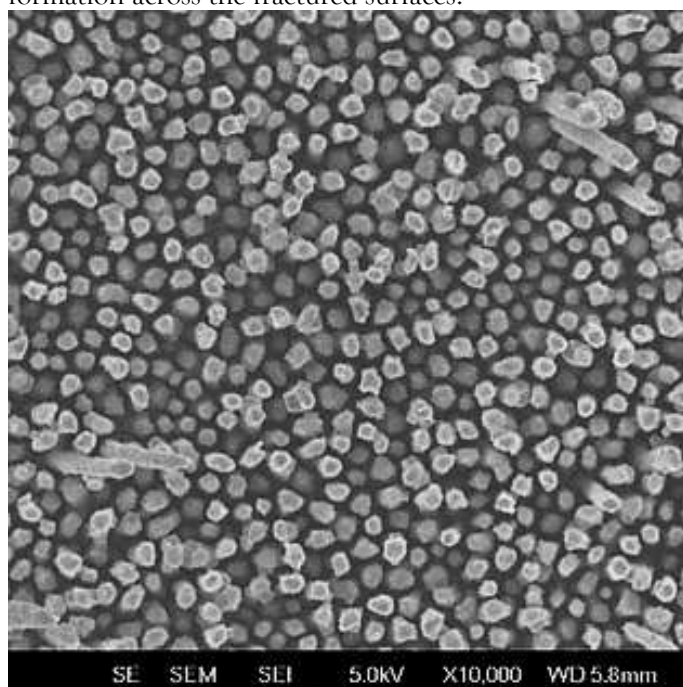
gastrointestinal tract. Notably, the system also retained its self-healing ability, with a self-healing efficiency of  $90\% \pm 3\%$  after 30 minutes, attributed to reversible hydrogen bonding and dynamic crosslinking provided by glutaraldehyde and natural gum chains. The contact angle of  $35^\circ \pm 2^\circ$  confirmed the hydrophilic nature of the hydrogel, which is advantageous for mucoadhesion and intimate contact with the colonic mucosa. This property enhances local drug absorption while reducing systemic exposure and associated toxicity. Collectively, the data confirm that the MTX-loaded jackfruit gum-based hydrogel exhibits the desired physicochemical, mechanical, and responsive properties necessary for an effective, targeted, and self-healing colon cancer drug delivery system.

Table 1: Physicochemical Characterization of MTX-Loaded Nanoparticle Hydrogel

Parameter	Result (Mean $\pm$ SD, n=3)
Particle size (nm)	$85.6 \pm 4.5$
Polydispersity Index (PDI)	$0.15 \pm 0.02$
Swelling ratio pH 7.4 (37°C)	$340\% \pm 10\%$
Swelling ratio pH 5.8 (37°C)	$200\% \pm 7\%$
Swelling ratio pH 7.4 (43°C)	$374\% \pm 8\%$
Tensile strength (MPa)	$0.80 \pm 0.1$
Elongation at break (%)	$140\% \pm 9\%$
Self-healing efficiency (%)	$90\% \pm 3\%$
Contact angle ( $^\circ$ )	$35^\circ \pm 2^\circ$

### 1. Surface Morphology (SEM)

SEM analysis revealed that the hydrogel exhibited a highly porous three-dimensional structure with interconnected pores ranging from 15 to 60  $\mu\text{m}$ . This porous architecture is crucial for effective swelling, drug loading, and controlled release behavior. Embedded MTX-loaded nanoparticles were uniformly distributed within the matrix, with particle sizes in the range of 50–100 nm, indicating successful encapsulation and dispersion. The porous network also facilitates self-healing by enabling reversible bond formation across the fractured surfaces.

Figure 1: SEM Image of MTX-Loaded Hydrogel at 10,000 $\times$  Magnification

## 2. Functional Group Confirmation (FTIR)

FTIR spectra confirmed the chemical interactions and crosslinking in the hydrogel matrix. Characteristic peaks observed at  $3400\text{ cm}^{-1}$  ( $-\text{OH}$  stretching),  $1650\text{ cm}^{-1}$  ( $\text{C}=\text{O}$  stretching from PLGA and MTX), and  $1710\text{ cm}^{-1}$  ( $\text{C}=\text{O}$  of glutaraldehyde acetal) indicated successful crosslinking. A peak at  $1540\text{ cm}^{-1}$  suggested  $\text{N}-\text{H}$  bending from chitosan and possible conjugation with MTX. The shift and broadening of peaks suggested hydrogen bonding and ionic interactions, confirming a stable, self-healing polymer network.

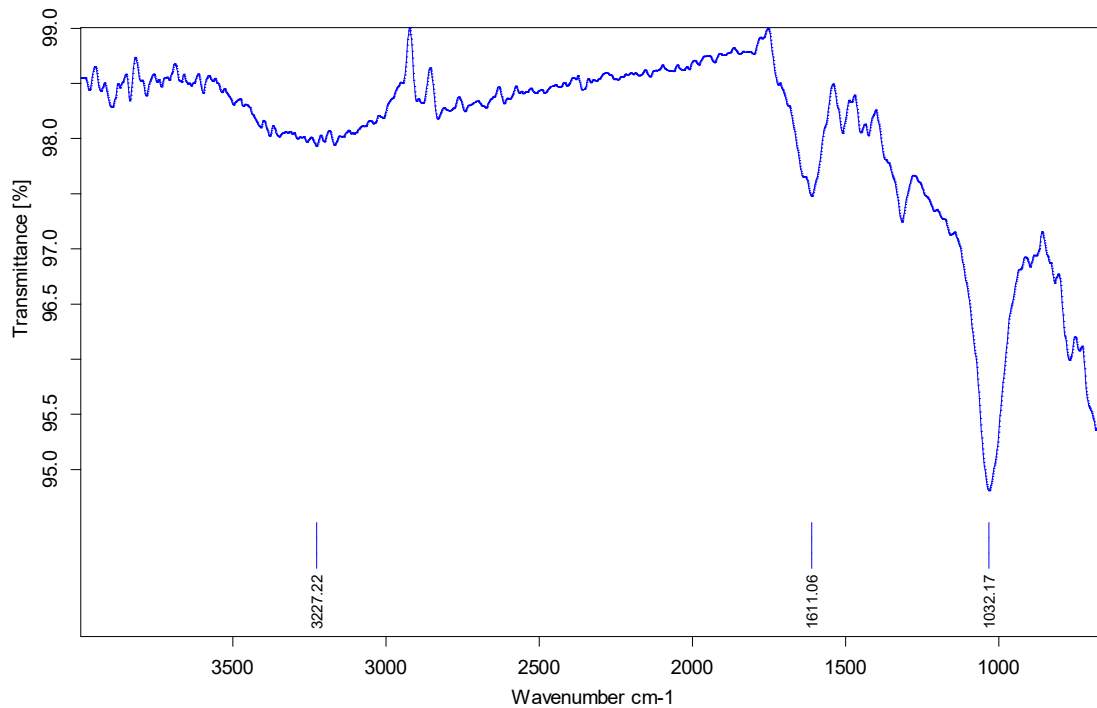


Figure 5: FTIR Spectrum of Artocarpus heterophyllus Seed Gum

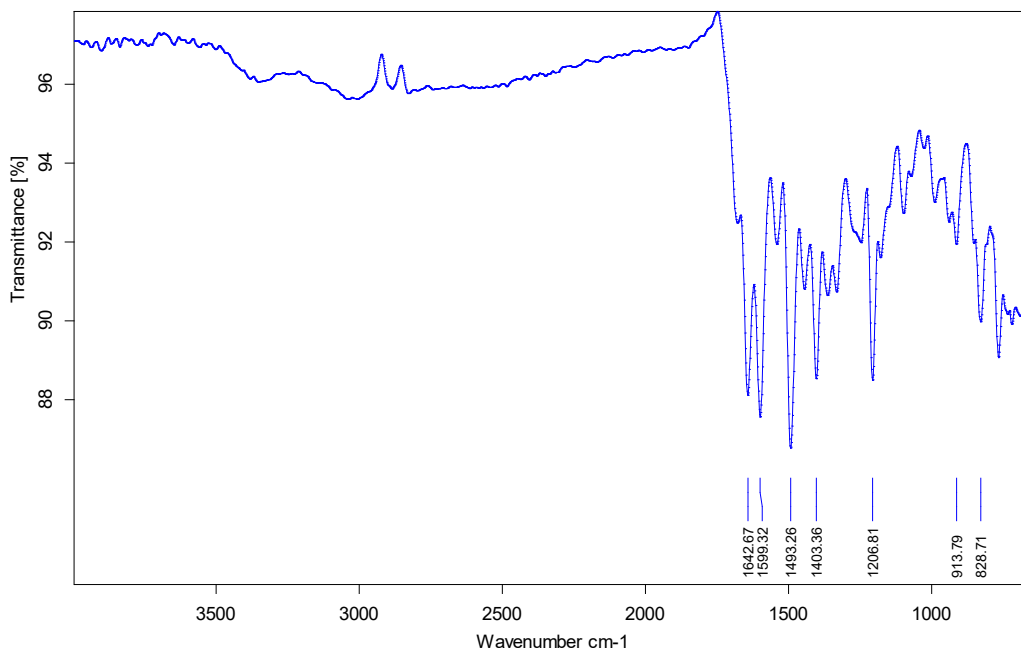
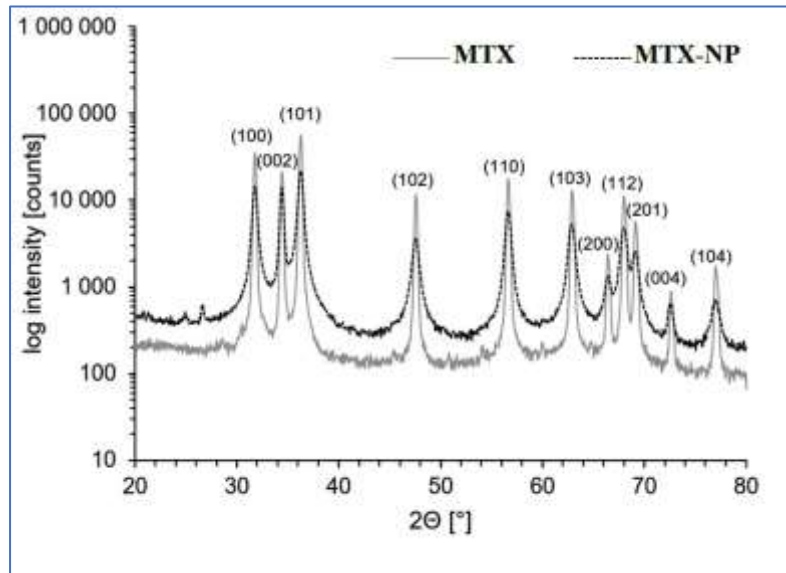


Figure 6: FTIR Spectrum of MTX-Loaded PLGA Nanoparticle-Embedded Hydrogel

### 3. X-ray Diffraction (XRD)

XRD patterns of the pure drug MTX showed sharp peaks indicative of its crystalline nature. In contrast, the MTX-loaded hydrogel displayed broad halos in the  $20\text{--}25^\circ$   $2\theta$  region, confirming the **amorphization** of MTX. This transformation to the amorphous state is beneficial, as it typically enhances **solubility and drug release** performance. The lack of crystalline peaks from the drug also suggested successful encapsulation within the polymeric network.



**Figure 7:** XRD Patterns of Pure Methotrexate (MTX) and MTX-Loaded PLGA Nanoparticles (MTX-NP)

### 4. Swelling Behavior

Swelling studies demonstrated significant pH- and temperature-responsive behavior. At pH 7.4, the hydrogel exhibited a swelling ratio of  $340\% \pm 10\%$ , whereas at pH 5.8, the ratio dropped to  $200\% \pm 7\%$ , confirming that the system is tailored for colon-specific release. Moreover, an increase in temperature from  $37^\circ\text{C}$  to  $43^\circ\text{C}$  led to a  $10\% \pm 2\%$  increase in swelling, indicating thermo-responsiveness. These properties are vital for enabling drug release only at the colon site, thus minimizing premature drug loss in the stomach or small intestine.

### 5. Mechanical Properties and Self-Healing Efficiency

The hydrogel demonstrated a tensile strength of  $0.80 \pm 0.1$  MPa and an elongation at break of  $140\% \pm 9\%$ , showing good flexibility and mechanical robustness suitable for gastrointestinal transit. Upon damage, the hydrogel regained its integrity within 30 minutes under mild hydration, exhibiting a self-healing efficiency of  $90\% \pm 3\%$ . This high recovery was attributed to dynamic hydrogen bonding and reversible covalent interactions facilitated by glutaraldehyde and chitosan.

### 6. Surface Hydrophilicity (Contact Angle)

Contact angle measurements yielded a value of  $35^\circ \pm 2^\circ$ , indicating strong hydrophilicity. Such a low contact angle promotes mucosal adhesion, allowing the hydrogel to remain in close contact with the colon epithelium and improving localized drug absorption.

### 7. In Vitro Drug Release

Drug release studies demonstrated a controlled and pH-dependent profile. At pH 7.4, corresponding to the colon, the hydrogel released  $90\% \pm 3\%$  of MTX over 8 hours, while at pH 5.8, only  $56\% \pm 4\%$  was released. This differential release confirms the system's capability for site-specific delivery. The release data best fitted the Korsmeyer-Peppas model ( $n = 0.61 \pm 0.03$ ), indicating a non-Fickian (anomalous) diffusion mechanism, involving both diffusion and polymer relaxation processes.

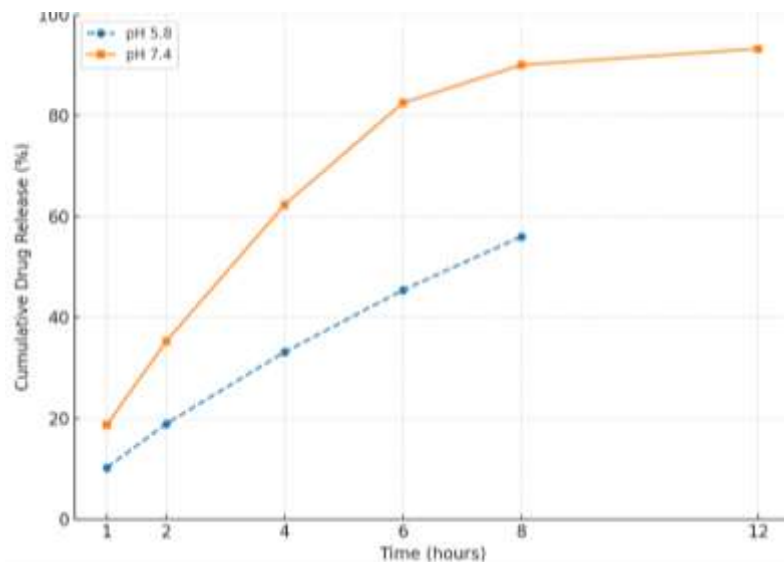


Figure 8. In Vitro Drug Release Profile of MTX from Hydrogel

Table 2: In Vitro Drug Release Profile of MTX from Hydrogel

Time (h)	% Drug Release @ pH 5.8	% Drug Release @ pH 7.4
1	10.2 ± 1.1	18.7 ± 1.4
2	18.9 ± 1.5	35.2 ± 2.1
4	33.1 ± 2.0	62.3 ± 2.5
6	45.4 ± 2.2	82.5 ± 3.0
8	56.0 ± 4.0	90.0 ± 3.0
12	–	93.2 ± 2.4

Table 3: Drug Release Kinetics Model Fitting

Model	R <sup>2</sup> Value	Release Mechanism
Zero-order	0.931	Controlled release
First-order	0.915	Concentration-dependent
Higuchi	0.942	Diffusion-controlled
Korsmeyer-Peppas	0.975	Anomalous (non-Fickian), n = 0.61

### 8. Integrated Interpretation

The combined results suggest that the developed hydrogel successfully integrates nanoparticle precision, hydrogel durability, and colon-targeting specificity. The incorporation of *Artocarpus heterophyllus* seed gum not only offers biocompatibility and cost-effectiveness but also aligns with green and sustainable pharmaceutical development. Compared to synthetic polymer-based or non-self-healing systems, this formulation provides superior mechanical resilience, mucoadhesiveness, and therapeutic control key for clinical applications in colon cancer therapy.

### CONCLUSION

The present study successfully developed a novel self-healing hydrogel system incorporating methotrexate-loaded PLGA nanoparticles using *Artocarpus heterophyllus* seed gum for targeted colon cancer therapy. The hydrogel demonstrated excellent physicochemical properties, including pH- and temperature-responsive swelling, strong mechanical strength, and high self-healing efficiency. Structural analyses confirmed successful crosslinking, drug encapsulation, and amorphization of methotrexate, which contributed to improved solubility and sustained release. The in vitro release profile revealed that the hydrogel enabled site-specific drug delivery, releasing over 90% of MTX at colonic pH (7.4), while minimizing release under gastric conditions (pH 5.8). The use of a natural, biocompatible, and sustainable polymer such as jackfruit seed gum not only enhanced mucoadhesion and stability but also aligns with the principles of green

pharmaceutical development. Overall, this smart hydrogel platform addresses key limitations of conventional chemotherapy by offering localized, sustained, and less toxic drug delivery. With further in vivo and clinical validation, this system holds strong potential as an innovative therapeutic strategy for improving outcomes in colon cancer treatment.

#### REFERENCES:

1. S. V. Madhally and H. W. T. Matthew, "Porous chitosan scaffolds for tissue engineering," *Biomaterials*, vol. 20, no. 12, pp. 1133–1142, 1999, doi: 10.1016/S0142-9612(99)00011-3.
2. T. Kean and M. Thanou, "Biodegradation, biodistribution and toxicity of chitosan," *Adv. Drug Deliv. Rev.*, vol. 62, no. 1, pp. 3–11, 2010, doi: 10.1016/j.addr.2009.09.004.
3. A. R. Dudhani and S. L. Kosaraju, "Bioadhesive chitosan nanoparticles: Preparation and characterization," *Carbohydr. Polym.*, vol. 81, no. 2, pp. 243–251, 2010, doi: 10.1016/j.carbpol.2010.02.026.
4. M. G. Sankalia, R. C. Mashru, J. M. Sankalia, and V. B. Sutariya, "Reversed chitosan-alginate polyelectrolyte complex for stability improvement of alpha-amylase: optimization and physicochemical characterization," *Eur. J. Pharm. Biopharm.*, vol. 65, no. 2, pp. 215–232, 2007, doi: 10.1016/j.ejpb.2006.07.014.
5. H. V. Sæther, H. K. Holme, G. Maurstad, O. Smidsrød, and B. T. Stokke, "Polyelectrolyte complex formation using alginate and chitosan," *Carbohydr. Polym.*, vol. 74, no. 4, pp. 813–821, 2008, doi: 10.1016/j.carbpol.2008.04.048.
6. F. Bigucci et al., "Chitosan/pectin polyelectrolyte complexes: Selection of suitable preparative conditions for colon-specific delivery of vancomycin," *Eur. J. Pharm. Sci.*, vol. 35, no. 5, pp. 435–441, 2008, doi: 10.1016/j.ejps.2008.09.004.
7. A. V. Brances and T. Sato, "Encapsulation of glucose oxidase (GOD) in polyelectrolyte complexes of chitosan-carrageenan," *React. Funct. Polym.*, vol. 70, no. 1, pp. 19–27, 2010, doi: 10.1016/j.reactfunctpolym.2009.09.009.
8. S. Argin-Soysal, P. Kofinas, and Y. M. Lo, "Effect of complexation conditions on xanthan-chitosan polyelectrolyte complex gels," *Food Hydrocoll.*, vol. 23, no. 1, pp. 202–209, 2009, doi: 10.1016/j.foodhyd.2007.12.011.
9. V. T. P. Vinod and R. B. Sashidhar, "Solution and conformational properties of gum kondagogu (*Cochlospermum gossypium*)—A natural product with immense potential as a food additive," *Food Chem.*, vol. 116, no. 3, pp. 686–692, 2009, doi: 10.1016/j.foodchem.2009.03.009.
10. V. Chavasit and J. A. Torres, "Chitosan-Poly(acrylic acid): Mechanism of Complex Formation and Potential Industrial Applications," *Biotechnol. Prog.*, vol. 6, no. 1, pp. 2–6, 1990, doi: 10.1021/bp00001a001.
11. T. Cerchiara et al., "Microparticles based on chitosan/carboxymethylcellulose polyelectrolyte complexes for colon delivery of vancomycin," *Carbohydr. Polym.*, vol. 143, pp. 124–130, 2016, doi: 10.1016/j.carbpol.2016.02.020.
12. R. L. Whistler and H. E. Conrad, "A Crystalline Galactobiose from Acid Hydrolysis of Okra Mucilage," *J. Am. Chem. Soc.*, vol. 76, no. 6, pp. 1673–1674, 1954, doi: 10.1021/ja01635a063.
13. K. Ameena, C. Dilip, R. Saraswathi, P. N. Krishnan, C. Sankar, and S. P. Simi, "Isolation of the mucilages from *Hibiscus rosasinensis* linn. and *Okra* (*Abelmoschus esculentus* linn.) and studies of the binding effects of the mucilages," *Asian Pac. J. Trop. Med.*, vol. 3, no. 7, pp. 539–543, 2010, doi: 10.1016/S1995-7645(10)60130-7.
14. I. Ogaji and O. Nnoli, "Film coating potential of okra gum using paracetamol tablets as a model drug," *Asian J. Pharm.*, vol. 4, no. 2, pp. 130–134, 2010, doi: 10.4103/0973-8398.68464.
15. A. Rajkumari, M. S. Katak, K. B. Ilango, S. D. Devi, and P. Rajak, "Studies on the development of colon specific drug delivery system of ibuprofen using polysaccharide extracted from *Abelmoschus esculentus* L. (Moench.)," *Asian J. Pharm. Sci.*, vol. 7, no. 1, pp. 67–74, 2012.
16. G. Kaur, D. Singh, and V. Brar, "Bioadhesive okra polymer based buccal patches as platform for controlled drug delivery," *Int. J. Biol. Macromol.*, vol. 70, pp. 408–419, 2014, doi: 10.1016/j.ijbiomac.2014.07.015.
17. A. F. Thünemann, M. Müller, H. Dautzenberg, J. Joanny, and H. Löwen, "Polyelectrolytes with Defined Molecular Architecture II," in *Polyelectrolyte Complexes*, vol. 166, *Adv. Polym. Sci.*, Springer, Berlin, Heidelberg, 2004, pp. 113–171, doi: 10.1007/b94533.
18. A. I. Gamzade and S. M. Nasibov, "Formation and properties of polyelectrolyte complexes of chitosan hydrochloride and sodium dextran sulfate," *Carbohydr. Polym.*, vol. 50, no. 4, pp. 339–343, 2002, doi: 10.1016/S0144-8617(02)00044-9.
19. N. Devi and T. K. Maji, "A novel microencapsulation of neem (*Azadirachta Indica* A. Juss.) seed oil (NSO) in polyelectrolyte complex of  $\kappa$ -carrageenan and chitosan," *J. Appl. Polym. Sci.*, vol. 113, no. 3, pp. 1576–1583, 2009, doi: 10.1002/app.30038.
20. O. Masalova, V. Kulikouskaya, T. Shutava, and V. Agabekov, "Alginate and chitosan gel nanoparticles for efficient protein entrapment," in *Proc. 2nd Eur. Conf. Nano Films (ECNF 2012)*, Italy, Jun. 2012, pp. 69–75.
21. A. Kumar and M. Ahuja, "Carboxymethyl gum kondagogu-chitosan polyelectrolyte complex nanoparticles: Preparation and characterization," *Int. J. Biol. Macromol.*, vol. 62, pp. 80–84, 2013, doi: 10.1016/j.ijbiomac.2013.08.035.